SIMULATION OF THE THERMOSPHERIC TIDES BY USE OF THE NCAR THERMOSPHERIC GENERAL CIRCULATION MODEL

C. G. Fesen, R. E. Dickinson, and R. G. Roble
National Center for Atmospheric Research
P.O. Box 3000
Boulder, CO 80307

Numerical calculations of the thermospheric tidal winds and temperatures were produced by use of the NCAR Thermospheric General Circulation Model (TGCM). The present calculations were restricted to solar minimum equinox conditions. The effects of viscosity, conductivity, diffusion, ion drag, winds, and temperature gradients were included. The semidiurnal propagating waves excited by heating in the lower atmosphere were modelled by use of the classical tidal perturbations as lower boundary conditions. The TGCM was tuned by adjusting the tidal forcing term until calculated semidiurnal winds and temperatures matched incoherent scatter observations. The tidal TGCM results are consistent with previous theoretical work and successfully reproduce high altitude temperature and velocity data, but give somewhat lower magnitudes for velocities and temperatures near 160 km than are seen observationally. Future plans call for similar studies being done for solar maximum equinox conditions, and then the solstice cases. These studies would benefit enormously from additional data, particularly if higher order modes are to be accurately included.

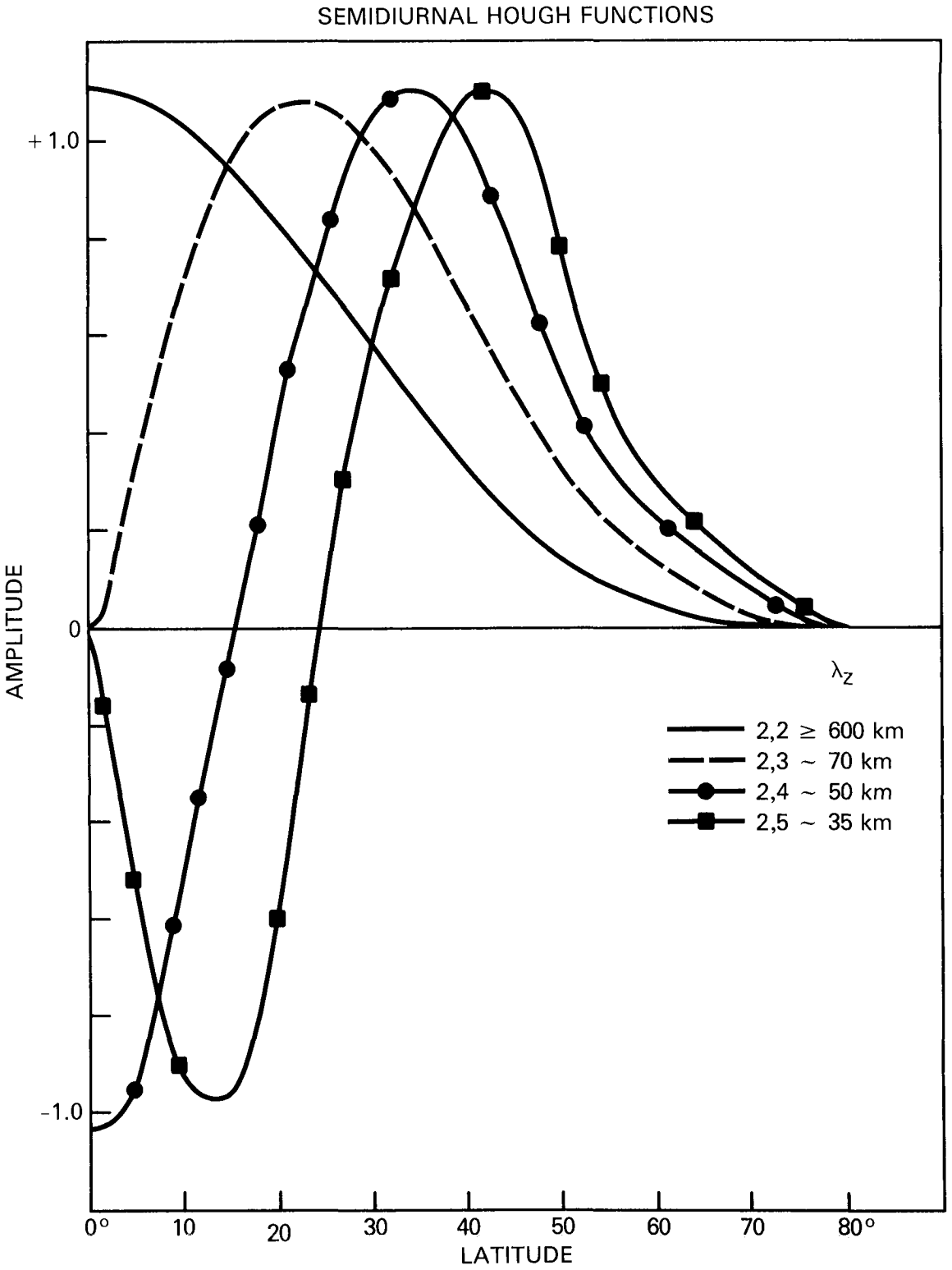

Figure 1. Classical Hough functions for the semidiurnal tides. Note increasing latitude structure for higher order modes.

$$G(Z, \Theta, t) = \sum_{n} L_n(Z)\, \Theta_n(\Theta)\, e^{i(\sigma t + s\lambda)}$$

FOR SEMIDIURNAL TIDES

$$\sigma = \frac{2\pi}{Y_2}$$

$$S = 2$$

$$\Phi_{97} = \left\{ \Phi_{2,2_{97}}\, \Theta_{2,2}\, e^{ik_{2,2} Z_{97}} + \Phi_{2,4_{97}}\, \Theta_{2,4}\, e^{i k_{2,4} Z_{97}} \right\} \bullet e^{i(4\pi t + 2\lambda)}$$

Figure 2. Classical solutions for any tidal variable as a function of altitude, latitude, and time can be written as shown in the top line of the figure. The geopotential Φ at 97 km can be written as shown.

1. SPECIFY THE GEOPHYSICAL CONDITIONS;

2. START WITH EQUILIBRIUM SOLUTIONS OF THE TGCM FOR SOLAR HEATING ALONE FOR THE APPROPRIATE CONDITIONS;

3. GUESS THE AMPLITUDE AND PHASE FOR THE 2,2 AND 2,4 GEOPOTENTIAL AT 97 KM, AND CALCULATE THE TOTAL TIDAL GEOPOTENTIAL AT 97 KM;

4. CALCULATE U, V, T AT 97 KM FROM THE GEOPOTENTIAL AT 97 KM USING FORMULAE FROM CHAPMAN AND LINDZEN AND USE THESE AS LOWER BOUNDARY CONDITIONS;

5. INTEGRATE THE MODEL EQUATIONS UNTIL EQUILIBRIUM IS ACHIEVED. THIS TYPICALLY TAKES 10½ MIN CRAY CPU;

6. FOURIER DECOMPOSE THE U, V, AND T FIELDS INTO ZONAL WAVENUMBERS 1 AND 2;

7. COMPARE THE TGCM U, V, AND T AMPLITUDES AND PHASES AT 18° AND 45° WITH OBSERVATIONS FROM ARECIBO, MILLSTONE HILL, AND SAINT SANTIN;

8. MODIFY THE INITIAL GUESSES FOR THE 2,2 AND 2,4 AMPLITUDES AND PHASES OF THE GEOPOTENTIAL AND REPEAT FROM STEP 4 UNTIL REASONABLE AGREEMENT IS OBTAINED BETWEEN THE MODEL AND OBSERVATIONS.

Figure 3. Steps in the calculation of the thermospheric winds and temperatures including the effect of tidal excitation.

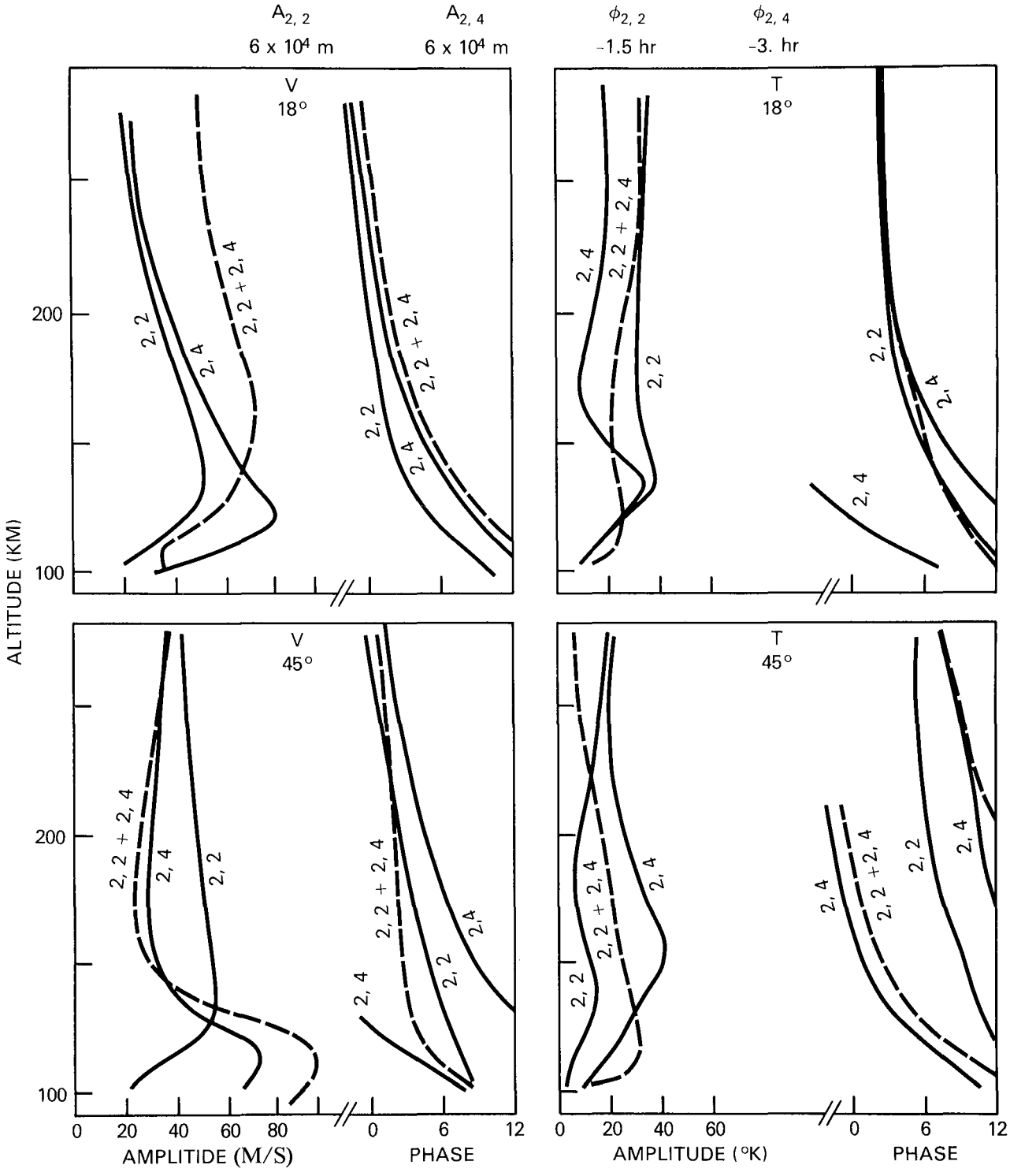

Figure 4. Results for a particular guess for the 2, 2 and 2, 4 components of the geopotential at 97 km.

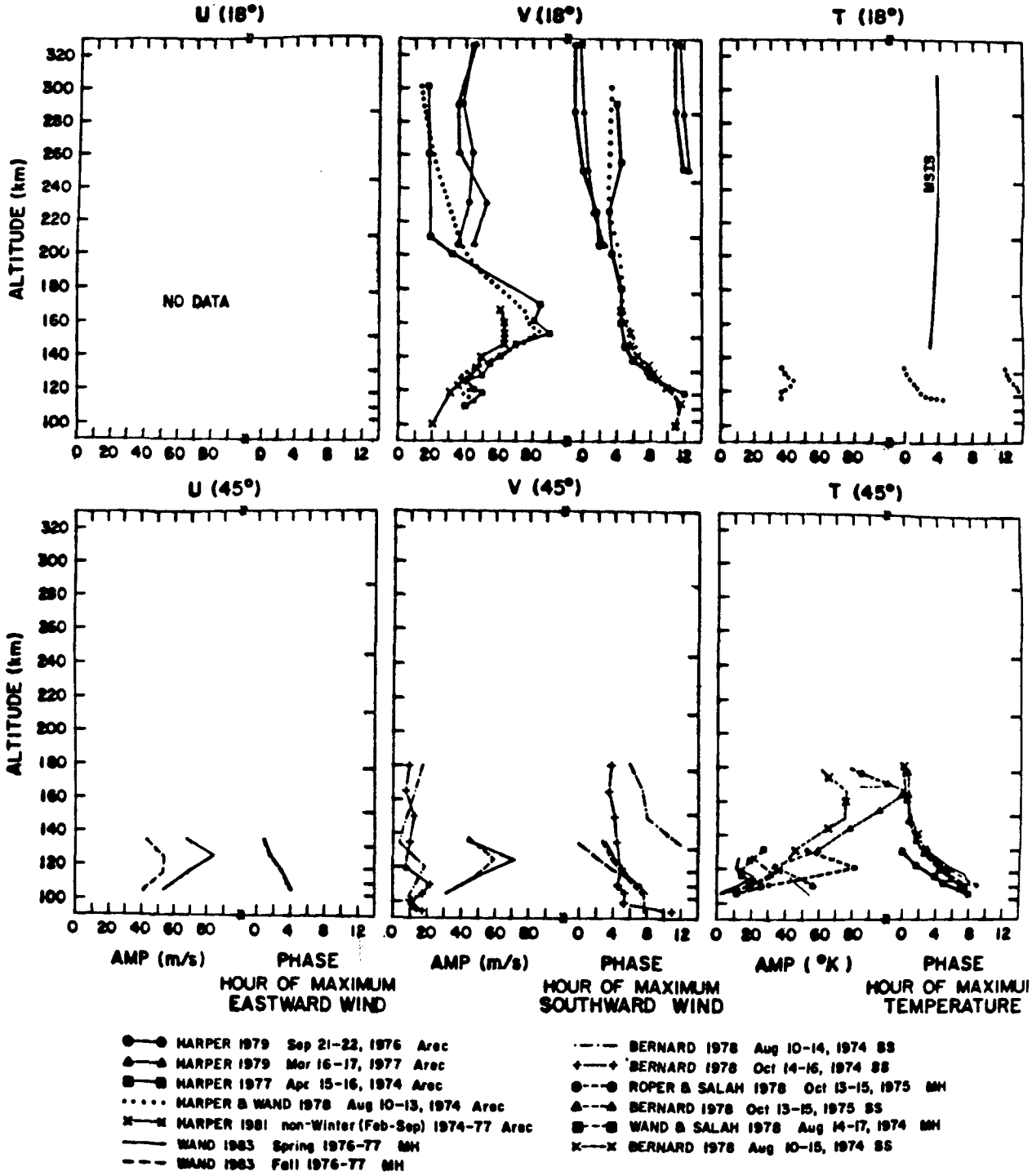

Figure 5. The incoherent scatter radar observations to which the TGCM winds and temperatures were compared.

BEST FIT TO OBSERVATIONS FOR
2, 2 AND 2, 4 GEOPOTENTIAL AT 97 KM:

$A_{2,2} = 4 \times 10^4$ m

$A_{2,4} = 3 \times 10^4$ m

$\phi_{2,2} = -0.5$ hr

$\phi_{2,4} = -2.5$ hr

Figure 6. The amplitudes and phases for the 2, 2 and 2, 4 geopotential at 97 km which best fit the observations shown in Figure 5.

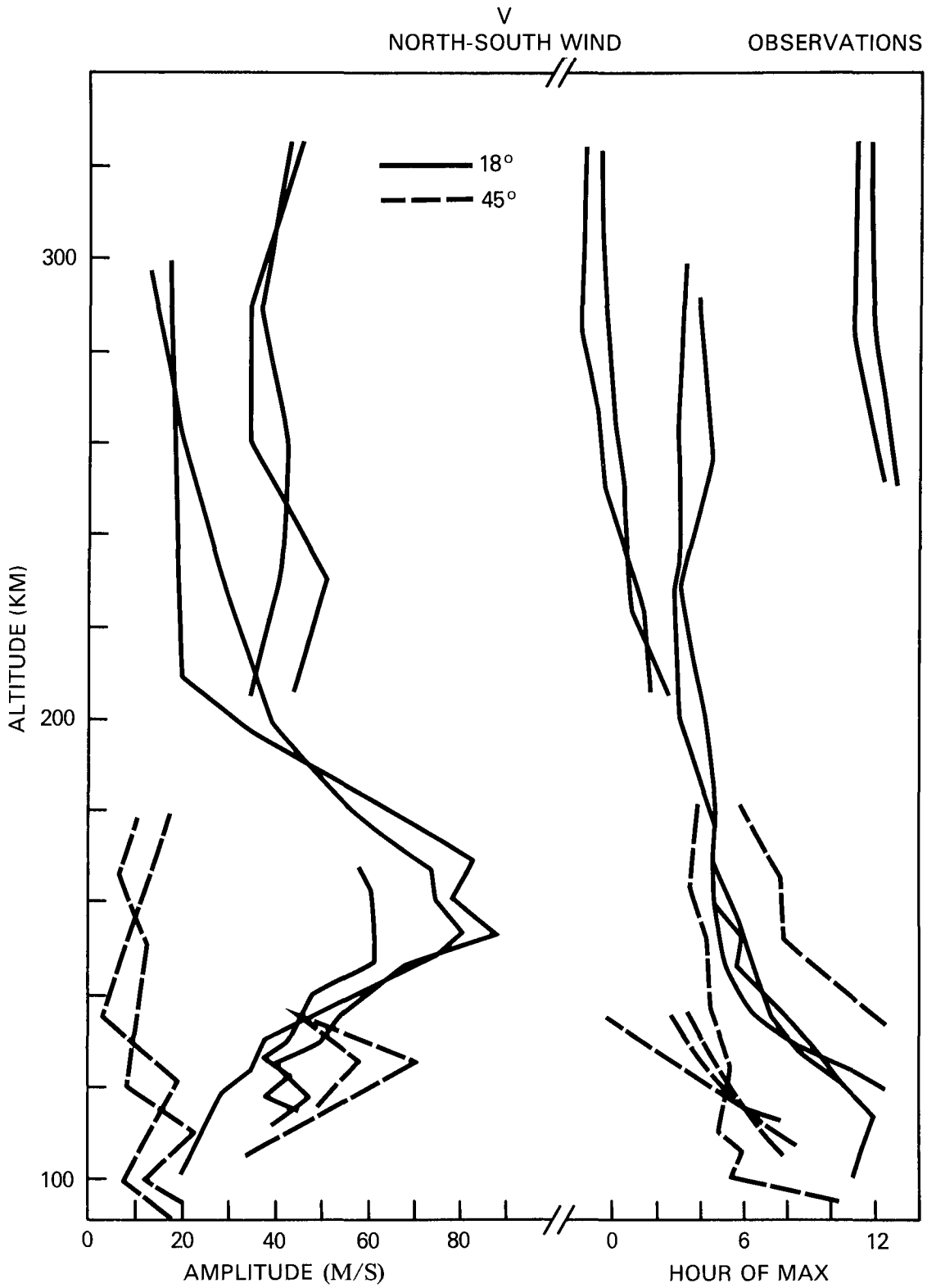

Figure 7. The north-south velocity observations at 18° and 45°.

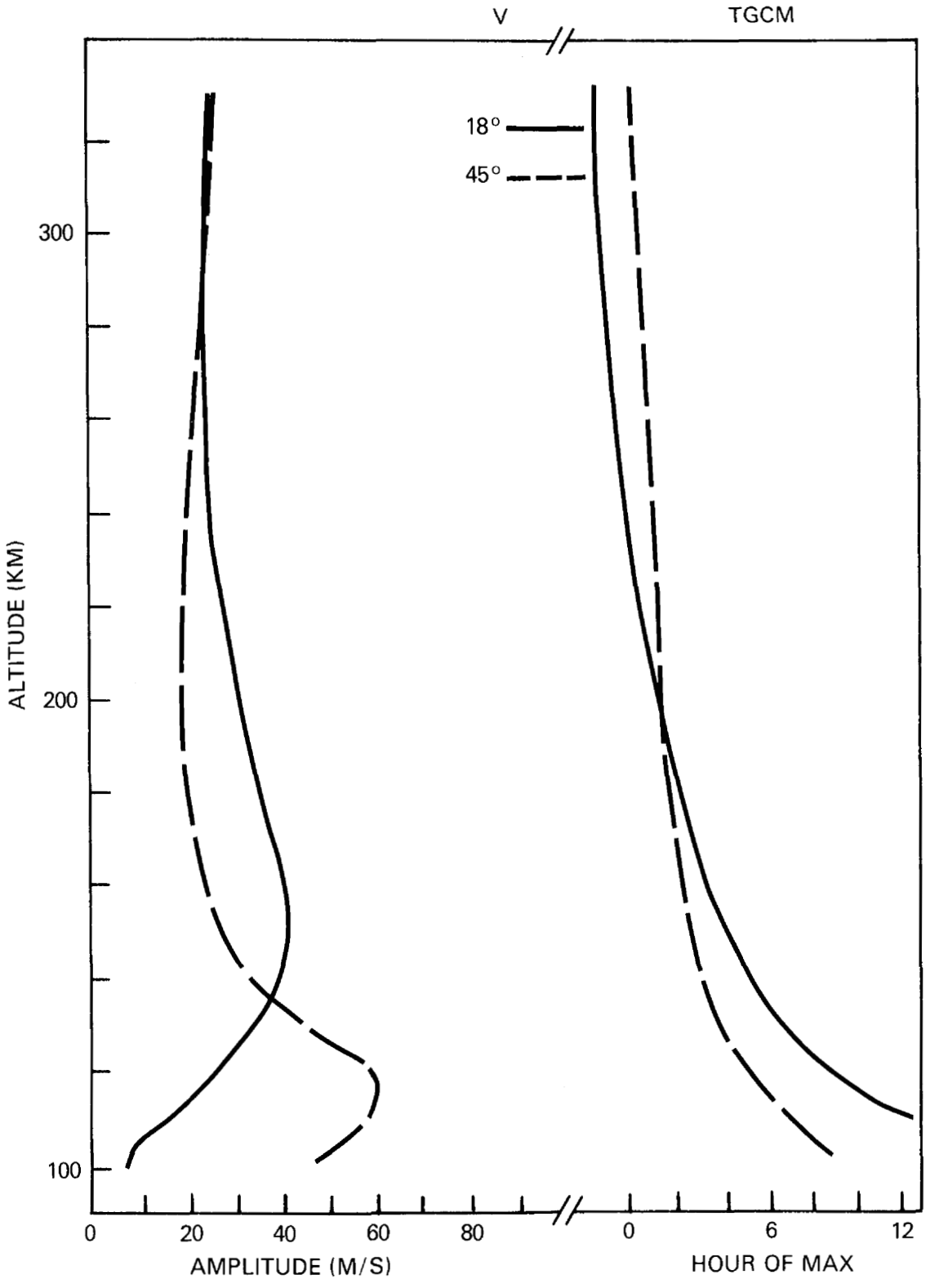

Figure 8. The TGCM north-south velocity at 18° and 45°.

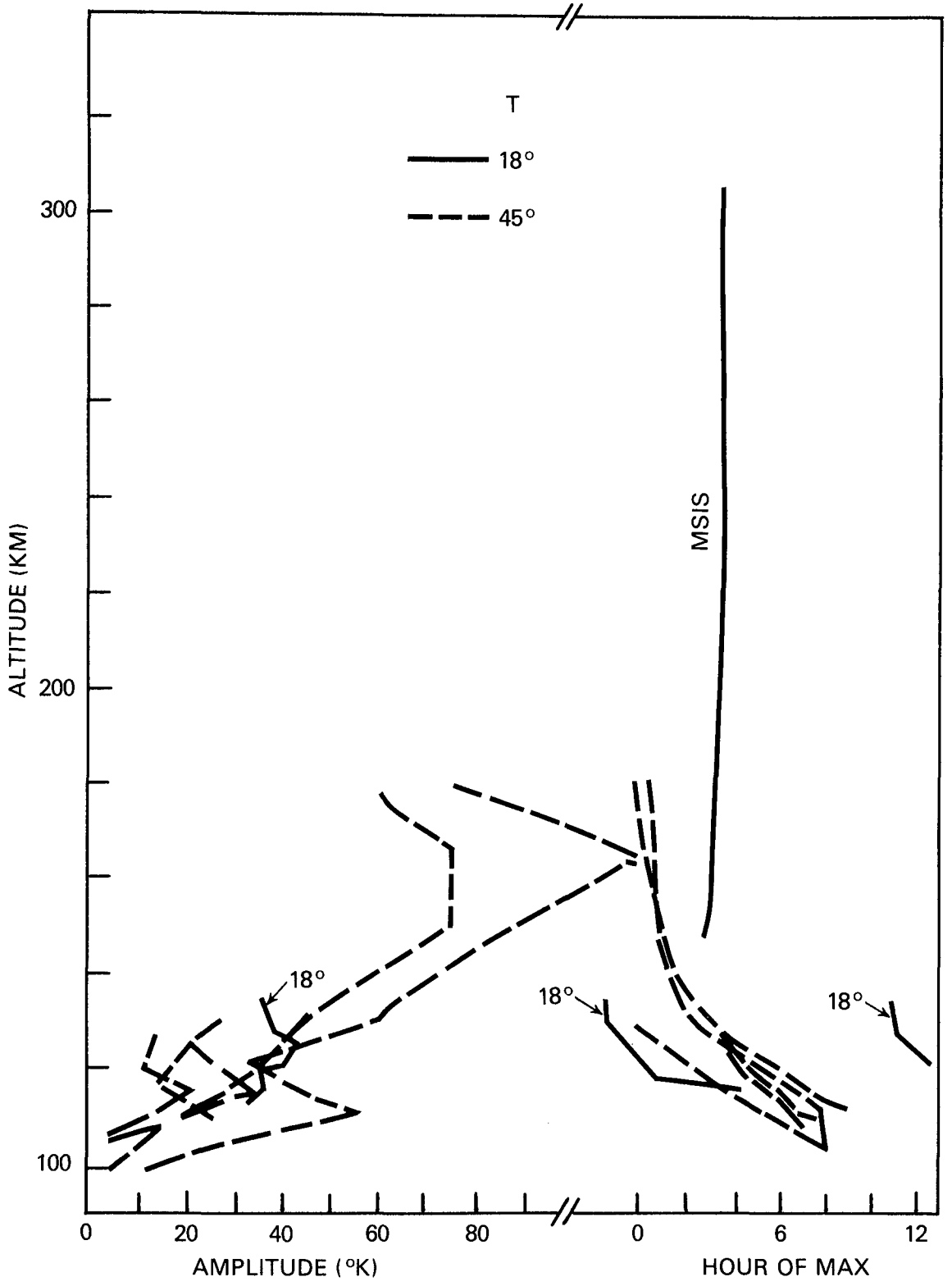

Figure 9. The temperature observations at 18° and 45°.

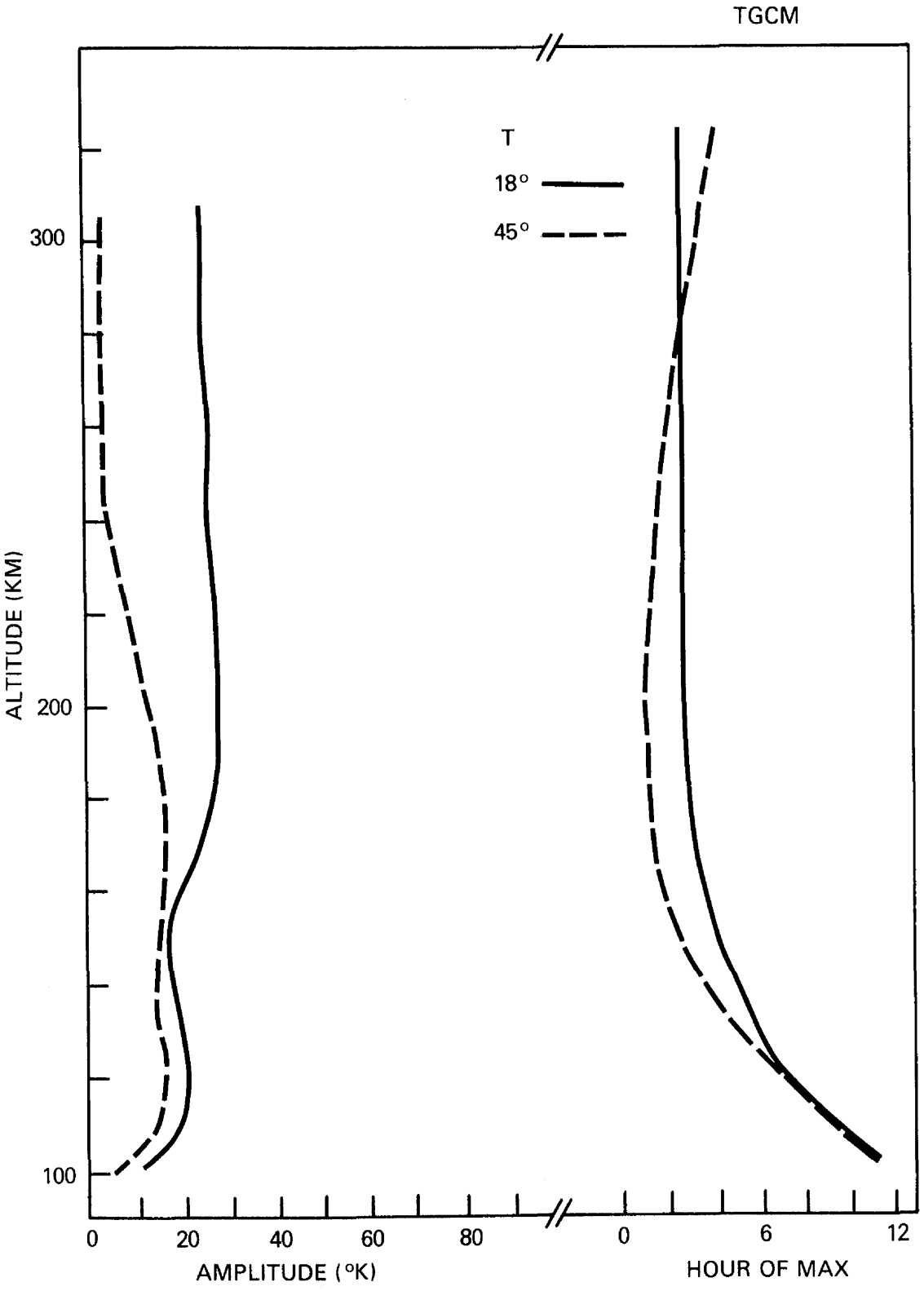

Figure 10. The TGCM temperatures at 18° and 45°.

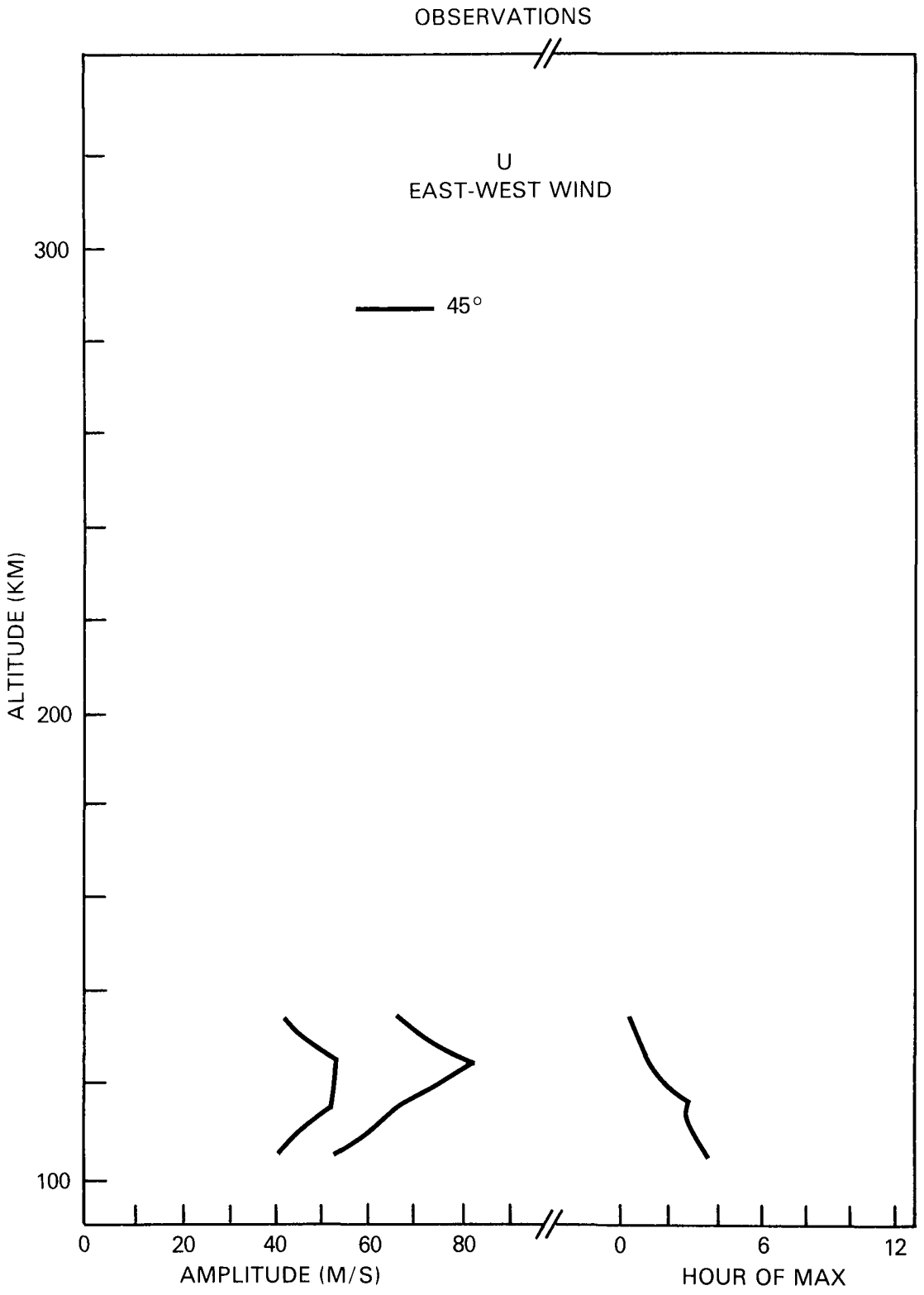

Figure 11. The east-west velocity observations at 45°.

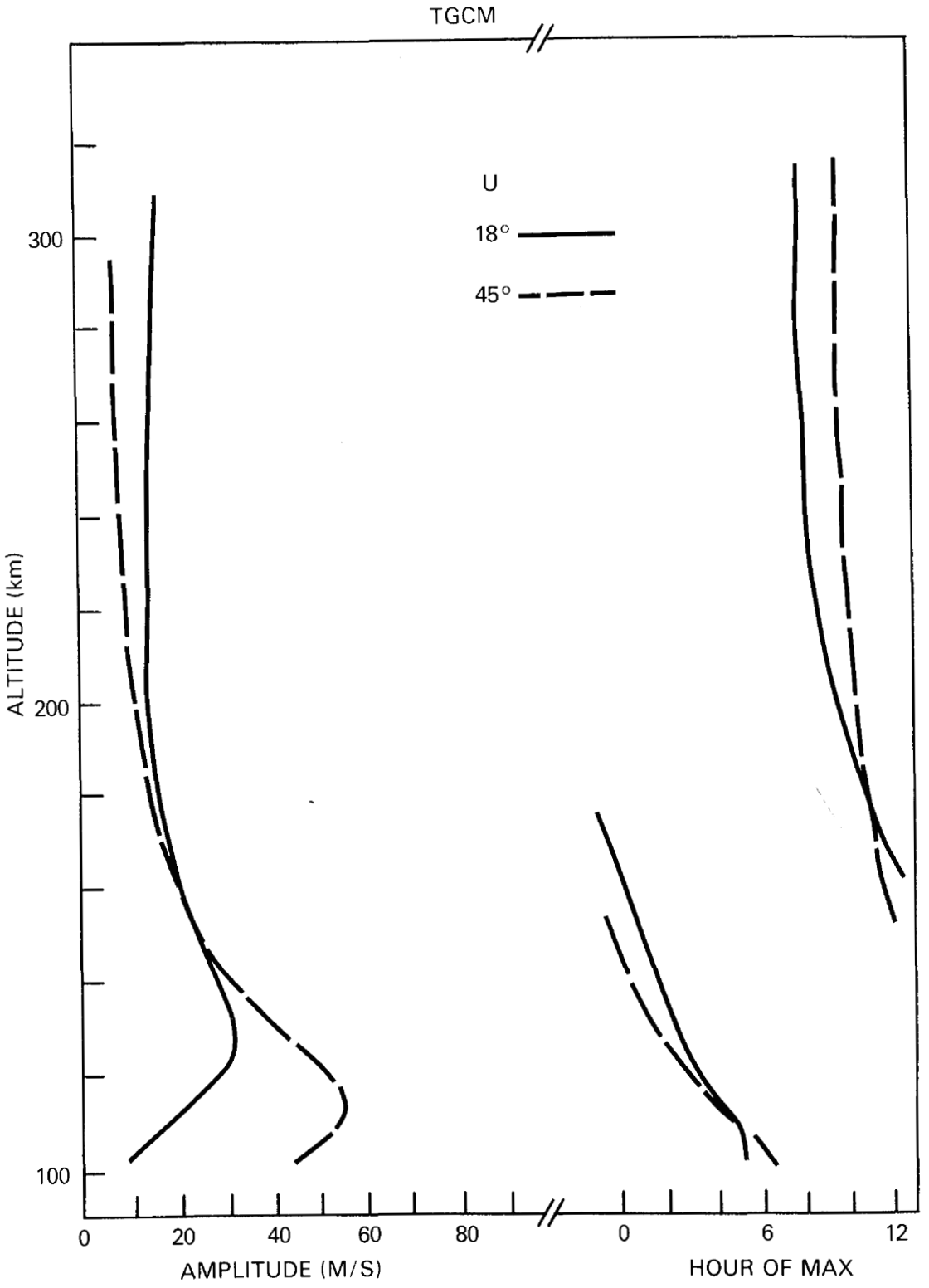

Figure 12. The TGCM east-west velocities at 18° and 45°.

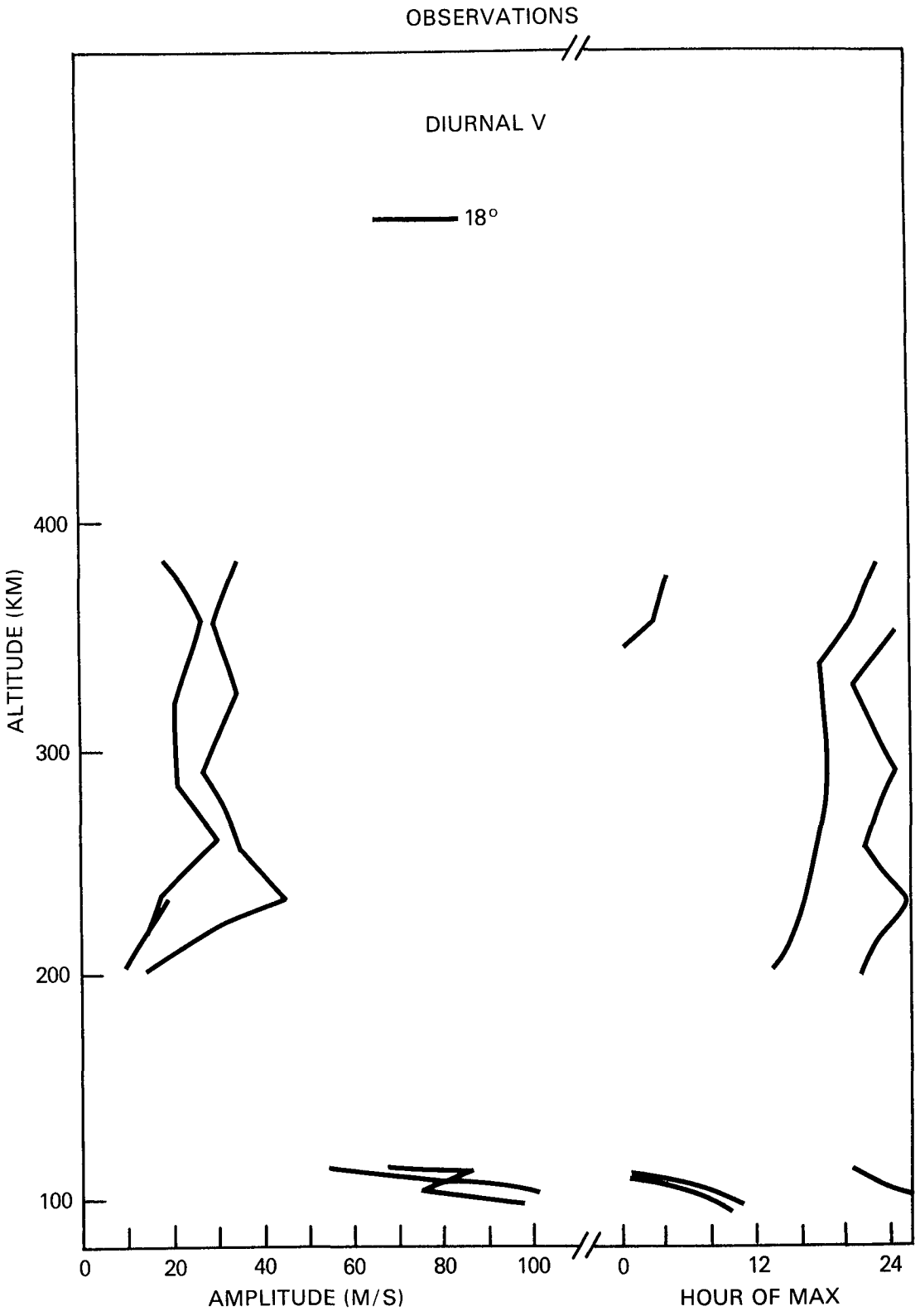

Figure 13. The diurnal north-south velocity observations at 45°.

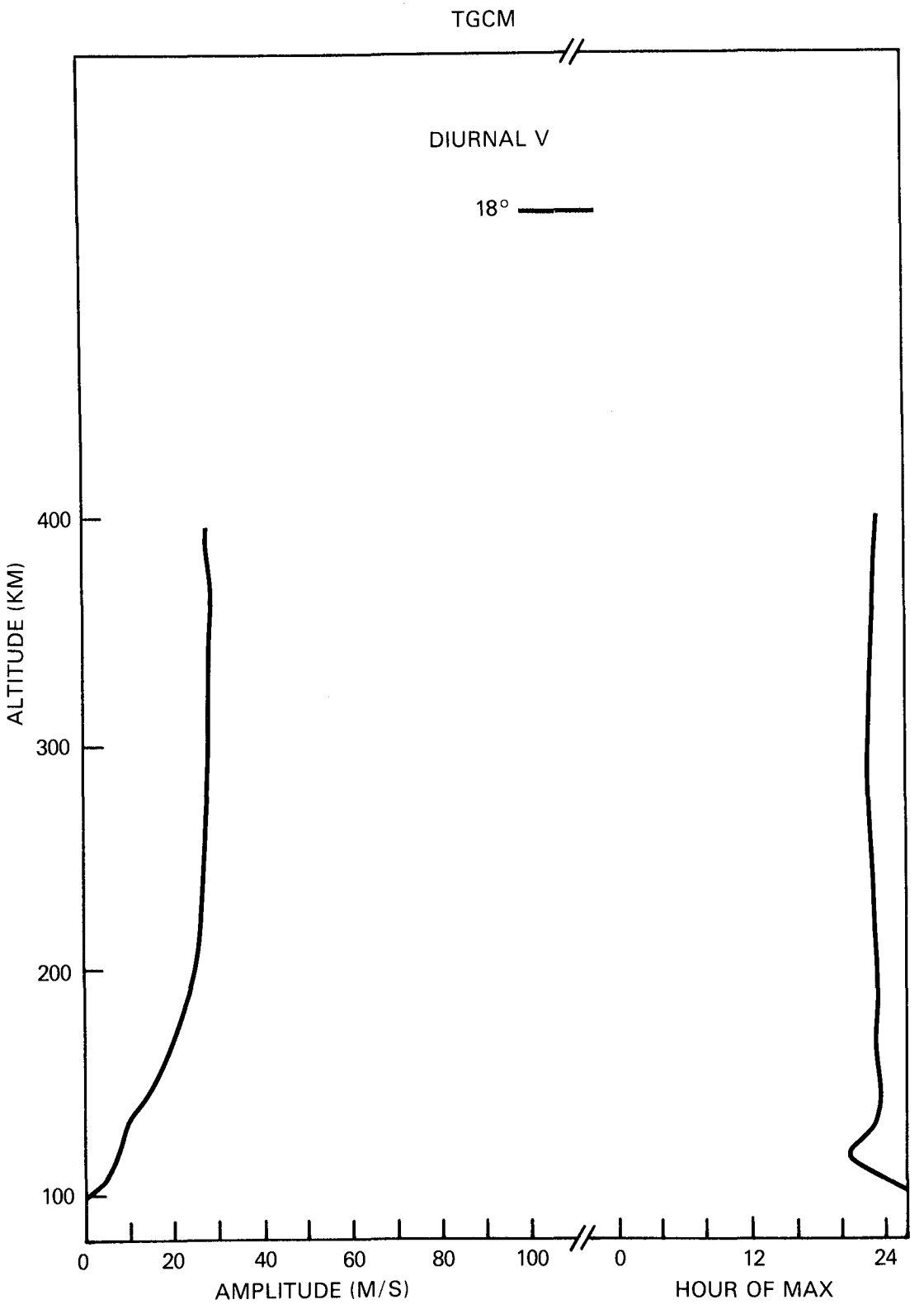

Figure 14. The TGCM diurnal north-south velocity results at 45°.